

Wire electrical discharge machining of AA7075/SiC/Al₂O₃ hybrid composite fabricated by inert gas-assisted electromagnetic stir-casting process

Shyam Lal · Sudhir Kumar · Z. A. Khan ·
A. N. Siddiquee

Received: 13 May 2013 / Accepted: 8 August 2013 / Published online: 22 August 2013
© The Brazilian Society of Mechanical Sciences and Engineering 2013

Abstract This paper investigated the effect of wire electrical discharge machining process parameters like discharge duration, pulse interval time, discharge current and the wire drum speed on the kerf width while machining newly developed hybrid metal matrix composite (Al7075/7.5 % SiC/7.5 % Al₂O₃). The hybrid composite was prepared by inert gas assisted electromagnetic stir-casting process. Taguchi method was used for parameter optimization and the level of importance was determined using analysis of variance. The results show that discharge duration, discharge current and wire drum speed were significant parameters. The discharge current was the most significant parameter that contributed maximum (47.16 %) to the kerf width followed by discharge duration (38.36 %), wire drum speed (5.16 %), and interaction, discharge duration × discharge peak current (5.47 %). The pulse interval time had insignificant effect on the kerf width. In confirmation test, the average experimental value of kerf width (228.7 μm) was within an error of 2.56 % of the predicted value at the optimum level of process parameters.

Keywords WEDM · Kerf width · Hybrid composite · Taguchi · ANOVA

1 Introduction

High-performance materials for aerospace applications and in the manufacturing sector, especially in the precision die industry, are supposed to have high strength, hardness and wear resistance. Metal matrix composites (MMCs) find applications in aerospace industry due to their light weight, high specific strength and good wear resistance [1]. Similarly, carbide ceramic materials used in the tool and die making are extremely hard and wear resistant [2]. SiC and Al₂O₃ are the ceramic reinforcements having high elastic modulus, compressive strength and hardness, whereas matrix alloy Al-7075 is a ductile metal. The use of traditional methods like milling, drilling and turning to machine ceramic-reinforced MMC or carbide ceramics causes serious tool wear. Also, machining the parts made of these materials conventionally place restrictions on the achieved dimensional stability. Wire electro discharge machining (WEDM) is an important and promising non-conventional machining process, which can be used to machine the electrically conductive work materials irrespective of their strength and hardness [3, 4]. There is no direct contact between the wire electrode and the work piece, thus the machined parts are not subjected to distortion. The dimensional accuracy of machined parts depends on the machining parameters and the part materials [5]. The most important performance measures in WEDM are material removal rate (MRR), surface roughness (SR) of machined surface and kerf, i.e., cutting width (K_f). The kerf determines the dimensional accuracy of the finished parts. The internal corner radius to be produced in WEDM operations is also limited by the kerf. The details of kerf produced in WEDM is shown in Fig. 1 [6].

The kerf is calculated by summing up the “wire diameter to 2× wire work piece gap distance”. The wire work

Technical Editor: Alexandre Mendes Abreu.

S. Lal · Z. A. Khan · A. N. Siddiquee
Mechanical Engineering Department, Jamia Millia Islamia,
New Delhi, India

S. Kumar (✉)
Noida Institute of Engineering and Technology, Gr. Noida, India
e-mail: s_k_tomar02@yahoo.com

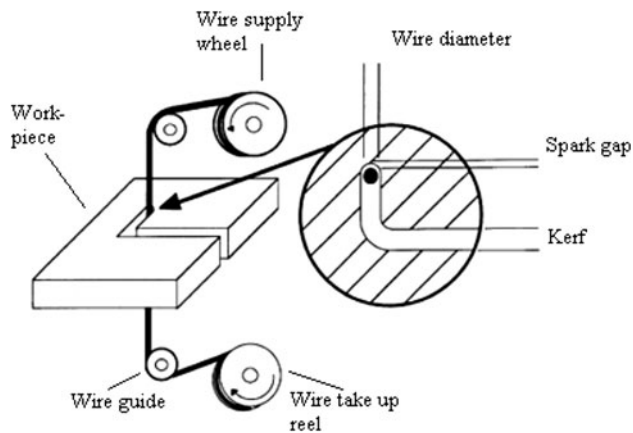


Fig. 1 Details of WEDM cutting gap [6]

piece gap usually ranges from 0.025 to 0.075 mm and is constantly maintained by a computer-controlled positioning system [7].

2 Literature survey

Tosun et al. [7] investigated the effect of WEDM machining parameters on the kerf and the MRR while machining AISI 4140 steel using the Taguchi method. The machining parameters were discharge duration, open circuit voltage, wire speed and dielectric flushing pressure. Based on the ANOVA method, the highly effective parameters on the kerf were open circuit voltage (OCV) and discharge duration. The wire speed and dielectric flushing pressure were less effective factors. The results showed that OCV contributed 63.44 % and the second-order ranking factor (discharge duration) contributed 28.7 % to the kerf. Increase in OCV and discharge duration increased the kerf width.

Yan et al. [8] examined the effect of WEDM machining parameter discharge duration on kerf (width of slit) while machining 10 and 20 vol % $\text{Al}_2\text{O}_3/6061$ Al composite. The experimental results revealed that the width of slit increased with increasing the discharge duration. The wire electrode wear rate (EWR) increases with increase in the percentage of reinforcing Al_2O_3 particles (0, 10, and 20 vol % of $\text{Al}_2\text{O}_3/6061$ Al). Also, it increased gradually as the discharge duration increased. The effects of process parameters including wire tension, flushing rate and wire speed of WEDM on wire breakage were investigated. A very low wire tension, a high flushing rate and a high wire speed are required to prevent wire breakage.

Parasher et al. [9] studied the effect of WEDM machining parameters such as gap voltage, discharge duration, pulse interval time, wire feed and the dielectric flushing pressure on kerf width while machining stainless

steel grade 304 L. The statistical and regression analysis of kerf was carried out using DOE. The results showed that discharge duration and the dielectric flushing pressure were the most significant factors, while gap voltage, pulse interval time and wire feed rate were less significant. The discharge duration, wire feed and flushing pressure had direct effect, while gap voltage and pulse interval time had reciprocal effect on the kerf width.

Shah et al. [10] investigated the effect of seven different WEDM process parameters on the machining responses, such as the MRR, kerf and surface roughness while machining tungsten carbide samples using the Taguchi method. Based on the study, the authors concluded that the material thickness has little effect on MRR and kerf, but was a significant factor for SR. Results of ANOVA showed that discharge duration and wire tension were the most significant factors for the kerf. The percentage contribution by discharge duration and wire tension was 39.64 and 26.47 %, respectively. Kerf increased with increase in discharge duration, but decreased with wire tension. Open voltage and pulse interval time affected kerf to a lesser degree.

Gupta et al. [11] evaluated the effect of WEDM process parameters on kerf width using the response surface methodology (RSM) while machining high-strength low alloy steel (HSLA). It was revealed from the results that kerf width decreased with increase in process parameters such as discharge duration, pulse interval time, spark gap voltage and discharge peak current. The analysis of results indicated that spark gap voltage, discharge duration, discharge peak current and pulse interval time had a significant effect on the kerf width.

Yang et al. [12] analyzed the variations in MRR, surface roughness and the corner deviation (CD) depending on parameters of the WEDM process in relation to the cutting of pure tungsten profiles. The analysis showed that CD decreased with an increase in wire tension when constant discharge duration was maintained. Also, CD decreases with an increase in the discharge duration when wire tension is held constant.

Patil and Brahmankar [13] experimentally investigated the effect of WEDM parameters on MRR, SR and the kerf width while machining $\text{Al}_2\text{O}_3/\text{AA} 6061$ composite. Taguchi orthogonal array (OA) was used in the study. It was found that reinforcement percentage, discharge current and discharge duration had significant effect on cutting rate, surface finish and kerf width. Increasing the discharge duration and discharge current was found to widen the kerf width, whereas it was low at low level of wire speed and high level of wire tension. Kerf width was also significantly influenced by the volume fraction of the ceramic particles and the lowest kerf width was associated with the highest volume fraction of alumina particles.

In the literature, few works have been reported regarding the machining of composites. The objective of the present work is to optimize the kerf width machining parameters of WEDM while machining newly developed AA7075/SiC/Al₂O₃ hybrid composite. The investigated machining parameters are discharge duration pulse interval time, discharge current and wire drum speed. ANOVA was used as the analytical tool in studying the effects of these machining parameters and their interaction effects. Also, the machined surfaces of hybrid composites were analyzed using SEM analysis.

3 Experimental procedure

3.1 Preparation of hybrid composite

In this study, the material employed is cast hybrid metal matrix composite fabricated using 15 wt% Al₂O₃ and SiC particulates (7.5 % each) in the metal matrix Al-7075 alloy. The aluminum alloy of 7xxx series has great potential to be utilized in aerospace and automotive industry because of its high strength to weight ratio and good resistance to corrosion. The composition of 7075 Al alloy is shown in Table 1.

Reinforcements SiC and Al₂O₃ in particulate form are used in the fabrication of hybrid composites. These reinforcements have 20–40 μm size particles and are used in combination in the ratio of 1:1. The melting of matrix metal Al-7075 alloy is carried out in a graphite crucible using electric resistance heating type muffle furnace. The de-gassing of melt is done by inert gas (Argon) for 10 min time before introduction of reinforcement into it. Also, an inert gas atmosphere is maintained above the melt surface during the synthesis of the hybrid composite, so as to minimize the contamination of aluminum due to atmospheric air. Now, when melting is achieved at temperature 715 °C, the melt is quickly lifted from the furnace and placed inside the electromagnetic stirring device. The stirring system is switched on and a forced vortex is generated in the melt. The preheated reinforcement phase (Al₂O₃ + SiC) particulate at a controlled rate is inducted into the melt. The reinforcement material particulates (Al₂O₃ and SiC) are mixed thoroughly and preheated to a temperature of 900 °C. After reinforcement induction phase is completed, the electromagnetic stirring is continued till melt reaches a solidus state. Figure 2 shows the

microstructure of 15 wt% Al₂O₃ and SiC particulates (7.5 % each) in Al-7075 alloy metal matrix composite cast by inert gas-assisted electromagnetic stir-casting process. The reinforcement phase is found to be uniformly distributed in the metal matrix at optimum stirring time (Fig. 2a, b); however higher stirring time leads to void formation and clustering of reinforcement particles as in Fig. 2c, d.

3.2 Machining parameters and response

The four input process parameters, namely discharge duration, pulse interval time, discharge peak current and the wire drum speed, were chosen as process parameters to study their effects on kerf width produced while cutting the hybrid composite.

The ranges of these process parameters were selected on the basis of machine capability and the pilot experiments carried out using the one parameter at a time approach. Table 2 gives the levels of various parameters and their designations.

3.3 Design of experiment using the Taguchi method

To get optimum and accurate results, the design of experiments (DOE) technique is used to collect the data. The orthogonal array forms the basis of the experimental analysis in the Taguchi method [14]. The four control parameters, i.e., discharge duration (a), pulse interval time (b), discharge current (c) and the wire drum speed (d) at three levels were selected in this study. *L*₂₇ standard array was chosen and MINITAB 15 software was used to analyze the results.

3.4 Conduct of experiment

WEDM is a spark erosion process. The sparks are generated between the work piece and the wire electrode immersed in a dielectric fluid. The material is removed by a series of discrete sparks at the area to be machined through an electrothermal mechanism. The continuous flow of dielectric fluid flushes away the removed particles from the machined region. The response characteristic used is kerf or cutting width. The strength and hardness of the work materials are not factors in WEDM, but melting point of the work material is an important property. Thus, WEDM finds extensive use in machining of hard materials. The kerf or cutting width affects the dimensional stability of the machined parts. The rectangular specimens of 4-mm thickness were prepared from the midportion of the cast ingot. The length and width of the specimen was 70 × 30 mm giving sufficient run for the machine to make various cuts of 10-mm length according to DOE (Table 3). The top and bottom surfaces of the specimen were given a

Table 1 Composition of Al 7075 alloy

| Zn | Cu | Mg | Cr | Si | Ti | Fe | Al |
|------|------|------|------|------|------|------|---------|
| 5.65 | 1.78 | 2.51 | 0.27 | 0.36 | 0.19 | 0.48 | Balance |

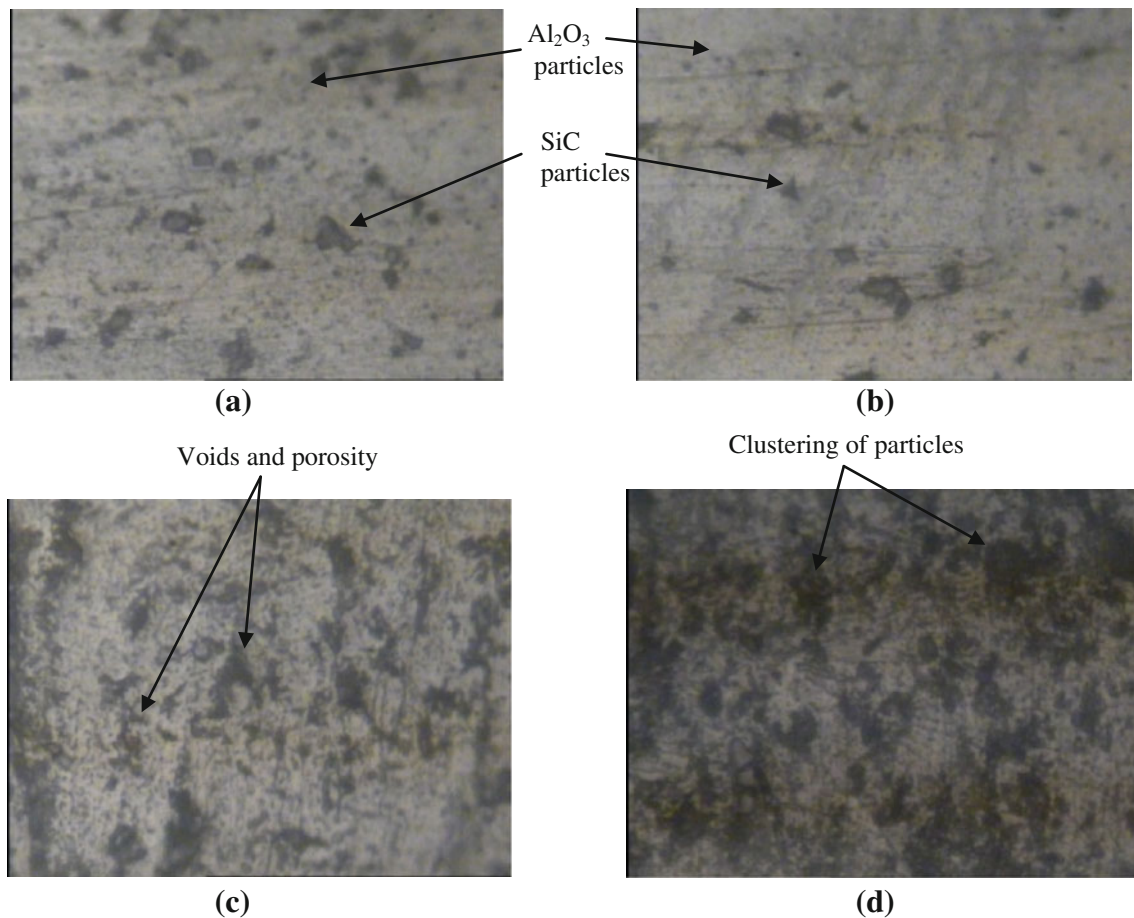


Fig. 2 a–d Microstructure of hybrid MMC containing 15 wt% Al₂O₃/SiC particulates (7.5 % each) in Al-7075 alloy

Table 2 Process parameters and their levels

| Symbol | Process parameter | Level 1 | Level 2 | Level 3 |
|--------|--------------------------------|---------|---------|---------|
| A | Discharge duration (μ s) | 4 | 10 | 16 |
| B | Pulse interval time (μ s) | 2 | 4 | 6 |
| C | Discharge current (amps) | 2 | 4 | 6 |
| D | Wire drum speed (m/min) | 4 | 6 | 8 |

smooth finish, using 600-grade emery papers. The wire EDM machine used was WEDM Programme and Control System Jiang Nan Saite NC, China. An electrode wire of molybdenum (0.18-mm diameter) was used. Deionised water was used as dielectric fluid at room temperature (30 °C). A photographic view of the wire electrical discharge machine is shown in Fig. 3. After machining, the specimens were cleaned with acetone. The kerf was measured using the focus tool makers' microscope ($\times 80$). To have a better average of the kerf width in each cut, this was measured at eight places spread over the entire length of cut, leaving 1-mm length at the beginning and 1 mm at the end. The specimen picture showing the WEDM cuts and

the kerf measurements made on different locations in a single cut are as in Fig. 4. In this study, the kerf values are the mathematical average of eight measurements made from the specimen in each cut. The microscope was interfaced with a computer and Caliper Pro 4.2 software was used for taking the kerf measurements. The observed average values of kerf width at different levels of the WEDM process parameters are as in Table 4.

3.5 Analysis of experiment

In the Taguchi method parameter design, the basic method converts the objective parameter to the signal to noise (S/N) ratio, which is treated as the quality characteristic evaluation index. The S/N ratio is used to measure the sensitivity of the quality characteristic being investigated in a controlled manner. In the Taguchi method, the term 'signal' represents the desirable effect (mean) for the output characteristic and the term 'noise' represents the undesirable effect (or signal disturbance) for the output characteristic which influences the outcome due to external factors, namely noise factors. The least variation and the

Table 3 Orthogonal array for L_{27}

| Experimental run | Control factors and levels | | | |
|------------------|----------------------------|---|---|---|
| | A | B | C | D |
| 1 | 1 | 1 | 1 | 1 |
| 2 | 1 | 1 | 2 | 2 |
| 3 | 1 | 1 | 3 | 3 |
| 4 | 1 | 2 | 1 | 2 |
| 5 | 1 | 2 | 2 | 3 |
| 6 | 1 | 2 | 3 | 1 |
| 7 | 1 | 3 | 1 | 3 |
| 8 | 1 | 3 | 2 | 1 |
| 9 | 1 | 3 | 3 | 2 |
| 10 | 2 | 1 | 1 | 1 |
| 11 | 2 | 1 | 2 | 2 |
| 12 | 2 | 1 | 3 | 3 |
| 13 | 2 | 2 | 1 | 2 |
| 14 | 2 | 2 | 2 | 3 |
| 15 | 2 | 2 | 3 | 1 |
| 16 | 2 | 3 | 1 | 3 |
| 17 | 2 | 3 | 2 | 1 |
| 18 | 2 | 3 | 3 | 2 |
| 19 | 3 | 1 | 1 | 1 |
| 20 | 3 | 1 | 2 | 2 |
| 21 | 3 | 1 | 3 | 3 |
| 22 | 3 | 2 | 1 | 2 |
| 23 | 3 | 2 | 2 | 3 |
| 24 | 3 | 2 | 3 | 1 |
| 25 | 3 | 3 | 1 | 3 |
| 26 | 3 | 3 | 2 | 1 |
| 27 | 3 | 3 | 3 | 2 |

optimal design are obtained by means of the S/N ratio. Quality characteristic ‘smaller the better (SB)’ is selected for kerf width. In the Taguchi method, a loss function is

defined to calculate the deviation between the experimental values and the designed values. Loss function value is further converted into S/N ratio. Minimizing quality loss is equivalent to maximizing the S/N ratio. The S/N ratio for kerf is given by expression.

$$\left(\frac{S}{N}\right)_{SB} = -10 \log \left[\frac{1}{n} \sum_{i=1}^n y_i^2 \right] \tag{1}$$

where y_i is the i th result of experiment and n is the repeated number of the i th experiment [14].

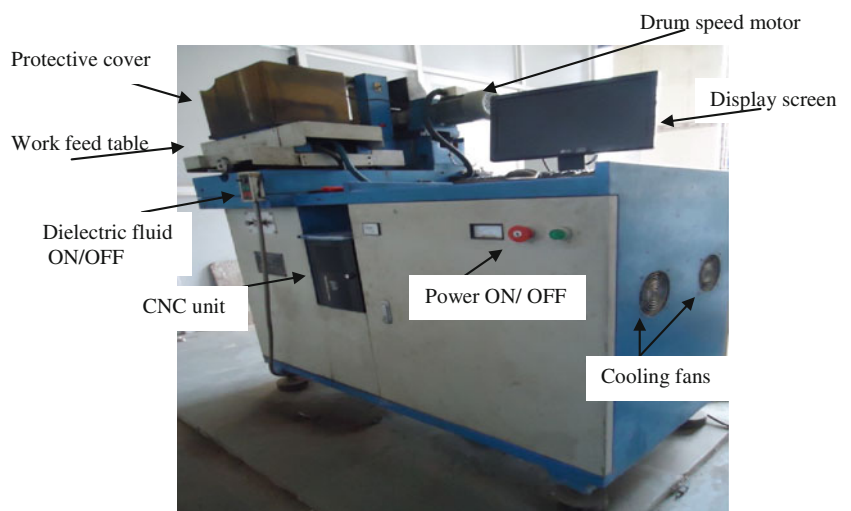
4 Results and discussion

The most important parameter describing the dimensional stability of machined components in WEDM is the kerf width. For a machined component, the dimensional tolerances are set to be in prescribed limits and can be achieved through proper study of the kerf width with respect to parameters. As the kerf determines the dimensional accuracy of the finished parts, for better dimensional accuracy the kerf width should be minimum.

4.1 Effect of process parameters on kerf width

Table 4 shows the average kerf width data. The analysis showed the effects of four main process parameters and their second-order interactions while cutting the hybrid composite. Based on the evidence at 95 % confidence level ($\alpha = 0.05$), discharge duration, discharge current and wire drum speed were found to have significant effect on kerf width (p value <0.05), whereas pulse interval time did not have significant effect (p value >0.05). Among the interactions, only the interaction between discharge duration and discharge current showed significant effect (p value

Fig. 3 Photographic view of wire electrical discharge machine



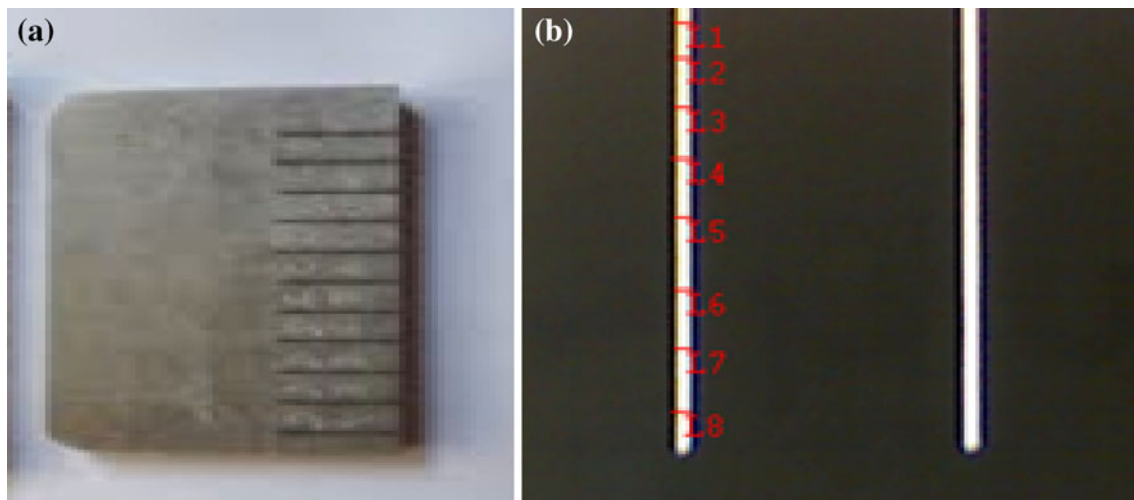


Fig. 4 a Cuts made on specimen by WEDM. b Kerf width measurements at various locations on a cut

Table 4 OA for L_{27} and observed values of kerf width for hybrid composite

| Exp. No. | Discharge duration (μ s) | Pulse interval time (μ s) | Discharge current (amps) | Wire drum speed (m/min) | Kerf width (μ m) |
|----------|-------------------------------|--------------------------------|--------------------------|-------------------------|-----------------------|
| 1 | 4 | 2 | 2 | 4 | 228 |
| 2 | 4 | 2 | 4 | 6 | 265 |
| 3 | 4 | 2 | 6 | 8 | 281 |
| 4 | 4 | 4 | 2 | 6 | 227 |
| 5 | 4 | 4 | 4 | 8 | 273 |
| 6 | 4 | 4 | 6 | 4 | 260 |
| 7 | 4 | 6 | 2 | 8 | 230 |
| 8 | 4 | 6 | 4 | 4 | 250 |
| 9 | 4 | 6 | 6 | 6 | 269 |
| 10 | 10 | 2 | 2 | 4 | 242 |
| 11 | 10 | 2 | 4 | 6 | 279 |
| 12 | 10 | 2 | 6 | 8 | 296 |
| 13 | 10 | 4 | 2 | 6 | 245 |
| 14 | 10 | 4 | 4 | 8 | 286 |
| 15 | 10 | 4 | 6 | 4 | 280 |
| 16 | 10 | 6 | 2 | 8 | 239 |
| 17 | 10 | 6 | 4 | 4 | 285 |
| 18 | 10 | 6 | 6 | 6 | 297 |
| 19 | 16 | 2 | 2 | 4 | 267 |
| 20 | 16 | 2 | 4 | 6 | 300 |
| 21 | 16 | 2 | 6 | 8 | 314 |
| 22 | 16 | 4 | 2 | 6 | 282 |
| 23 | 16 | 4 | 4 | 8 | 303 |
| 24 | 16 | 4 | 6 | 4 | 291 |
| 25 | 16 | 6 | 2 | 8 | 284 |
| 26 | 16 | 6 | 4 | 4 | 277 |
| 27 | 16 | 6 | 6 | 6 | 298 |
| | | | | | Average = 272.2 |

Table 5 Analysis of variance for SN ratios (kerf width) with interaction and pooling

| Source | DF | Seq SS | Adj SS | Adj MS | F | P | % Contribution |
|--|----|---------|--------|---------|-------|-------|----------------|
| Discharge duration | 2 | 6.4729 | 6.4729 | 3.23645 | 80.02 | 0.000 | 38.36 |
| Discharge current | 2 | 7.9581 | 7.9581 | 3.97907 | 98.38 | 0.000 | 47.16 |
| Wire drum speed | 2 | 0.872 | 0.872 | 0.43601 | 10.78 | 0.001 | 5.16 |
| Discharge duration × discharge current | 4 | 0.923 | 0.923 | 0.23076 | 5.71 | 0.005 | 5.47 |
| Residual error | 16 | 0.6472 | 0.6472 | 0.04045 | | | 3.84 |
| Total | 26 | 16.8733 | | | | | |

<0.05). Other interactions were not statistically significant. The data pooled and Table 5 show the pooled ANOVA for the kerf width. The percentage contribution of each parameter is calculated. The discharge current was the most significant parameter that contributed maximum (47.16 %) to the kerf width. The contribution from other parameters were discharge duration (38.36 %) and wire drum speed (5.16 %). The contribution from second-order interaction parameter (discharge duration × discharge current) was 5.47 %. The average S/N ratios and average mean values of kerf width for each parameter are shown in Tables 6 and 7. The mean responses refer to the average value of the performance characteristic for each parameter at different levels. The average values of kerf width for each parameter at levels 1, 2 and 3 are calculated and presented in Table 7. These values are plotted as in Fig. 5a. The main effects (raw data) of the various process parameters when they change from lower to higher levels (Table 7) can be visualized in Fig. 5b. The S/N ratio analysis suggests that the best levels for minimum value of kerf width are A_1, C_1, D_1 . The main effect plot for S/N ratio, mean and their interaction are shown in Figs. 5, 6 and 7 respectively.

4.1.1 Effect of discharge duration on kerf width

Figure 6a indicates the effect of discharge duration on the kerf width. The kerf width increases as the discharge duration increases. The influence of discharge duration on the kerf width is the second most significant parameter. In the WEDM process, the discharge energy produces very high temperature at the point where spark strikes the surface. This causes a minute part of specimen to melt and vaporize. Increasing the discharge duration means longer spark duration, i.e., more amount of discharge energy per spark reaching the surface. Because of this fact, a large amount of material melts per spark in the gap. This widens the gap. Thus, increase in the discharge duration is found to widen the kerf width. Hence, to obtain smaller kerf width, the discharge duration should be kept low. Results from this study are in agreement with those of other researchers [9, 13].

Table 6 Response table for signal to noise ratios (kerf width)

| Level | Discharge duration | Discharge current | Wire drum speed |
|-------|--------------------|-------------------|-----------------|
| 1 | −48.06 | −47.90 | −48.42 |
| 2 | −48.67 | −48.92 | −48.71 |
| 3 | −49.26 | −49.15 | −48.85 |
| Delta | 1.20 | 1.25 | 0.43 |
| Rank | 2 | 1 | 3 |

Table 7 Response table for means (kerf width)

| Level | Discharge duration | Discharge current | Wire drum speed |
|-------|--------------------|-------------------|-----------------|
| 1 | 253.7 | 249.3 | 264.4 |
| 2 | 272.1 | 279.8 | 273.6 |
| 3 | 290.7 | 287.3 | 278.4 |
| Delta | 37.0 | 38.0 | 14.0 |
| Rank | 2 | 1 | 3 |

4.1.2 Effect of discharge current on kerf width

Figure 6c represents the effect of discharge current on the kerf width. Discharge current is the most significant process parameter affecting the kerf. The kerf width increases as the discharge current increases. This is because the discharge energy becomes intense with increase in the discharge current. This high-intensity spark energy produces more powerful explosion resulting in a deeper crater being created on the surface. It is obvious that deeper craters will widen the kerf width. Hence, to obtain smaller kerf width, the discharge current should be kept low. Results from this study are in agreement with other researchers [7, 13].

4.1.3 Effect of wire drum speed on kerf width

Figure 6d shows the effect of wire drum speed on the kerf width. The kerf width increases as the wire drum speed increases. During machining of materials by WEDM, a large amount of molten metal and the

Fig. 5 Main effect plots for S/N ratio (kerf width)

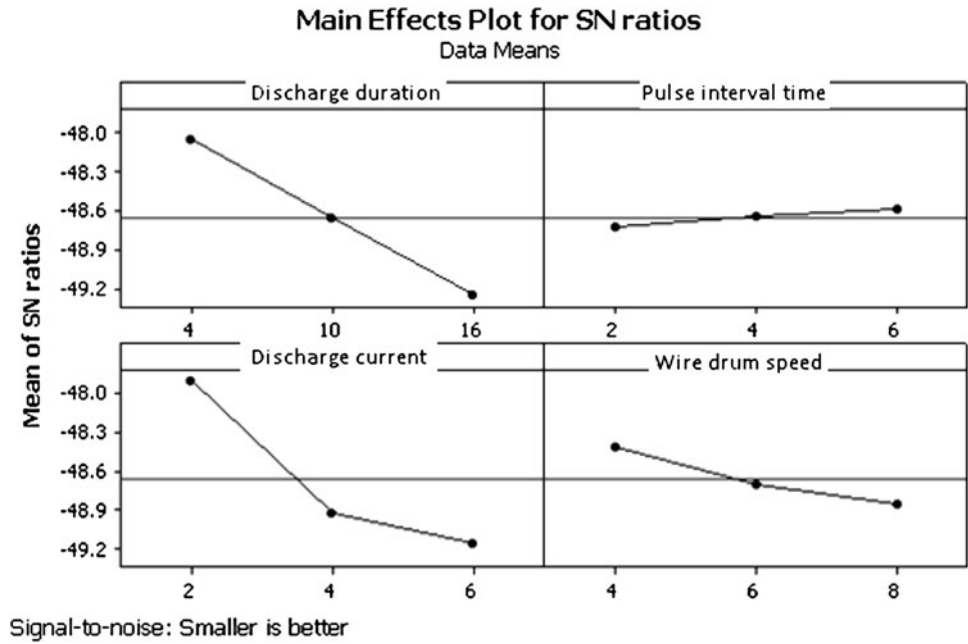
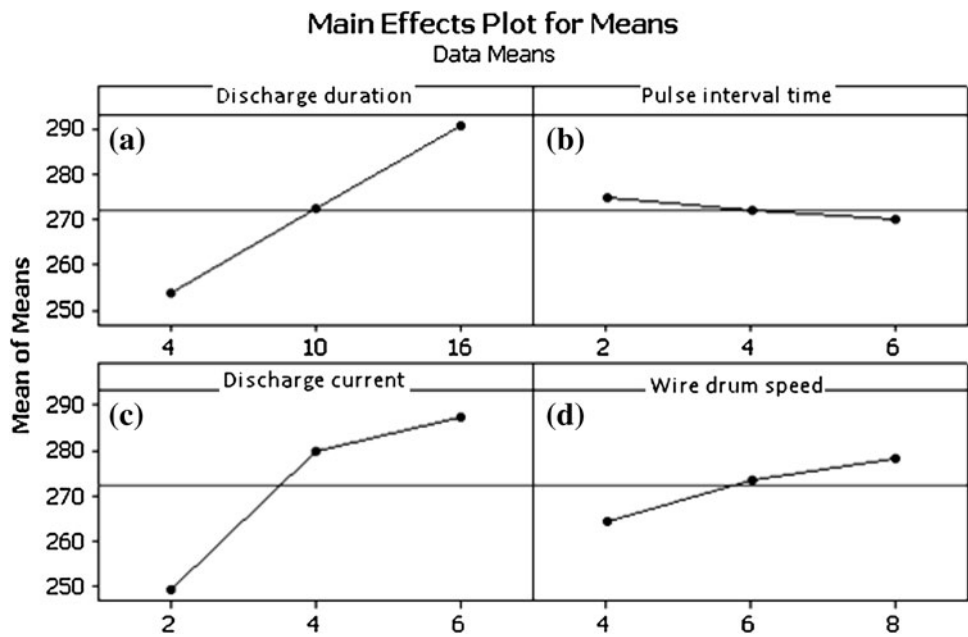


Fig. 6 a–d Main effect plots for means (kerf width)

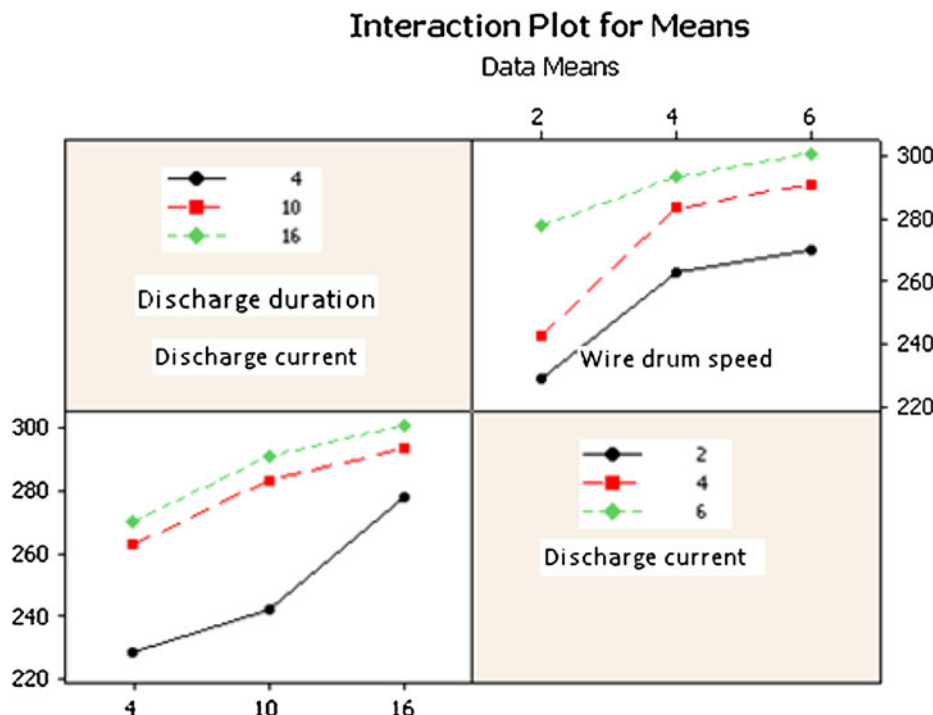


reinforcement particles (due to intense spark energy) are available in the gap as debris. The effective flushing of this debris material will add to kerf width. The high wire drum speed helps in effective flushing of molten metal. Ineffective flushing may contaminate the gap and thicken the recast layer. Hence, kerf width is higher at higher wire drum speed and low at low wire drum speed. Results from this study are in agreement with those of other researchers [9, 13].

4.1.4 Effect of pulse interval time on kerf width

Figure 6b indicates the effect of pulse interval time on the kerf. Although this is not a significant factor contributing to the kerf width, the response graph trends can be explained as follows. The kerf width decreases as the pulse interval time increases. This is because increasing the pulse interval time means that less number of discharges occur for a specific period of time, resulting in a small quantity of

Fig. 7 Interaction plot for S/N ratio on kerf width



metal melting in the gap. This produces lower kerf width. Results from this study are in agreement with those of another researcher [9].

Figure 7 illustrates the interaction plot between discharge duration and discharge peak current. The plot reveals that discharge peak current has a larger effect on kerf width than that of discharge duration.

4.2 Estimation of optimum performance characteristic

The optimum value of kerf width is predicted at the selected levels of significant parameters. The significant process parameters and their optimum levels are chosen from the response graph as A_1 , C_1 , D_1 , i.e., discharge duration at 4 μs , discharge current level at 2 amps and wire drum speed at 4 m/min.

The estimation mean of response characteristic can be computed as [14]

$$\mu_{kf} = K_f + (A_1 - K_f) + (C_1 - K_f) + (D_1 - K_f)$$

where K_f is the overall mean of kerf width ($K_f = 272.2 \mu\text{m}$).

$$\mu_{kf} = 253.7 + 249.3 + 264.4 - 2(272.2) = 223.0 \mu\text{m}$$

The estimate of the mean (μ_{kf}) is only a point estimate based on the average of results obtained from the experiment. Statistically, this provides a 50 % chance of the true average being greater than μ_{kf} . It is therefore customary to represent the values of a statistical parameter as a range

within which it is likely to fall for a given level of confidence [14]. This range is termed as the confidence interval (CI). In other words, the confidence interval is a maximum and minimum value between which the true average should fall at some stated percentage of confidence [14].

The confidence interval of the predicted mean for the confirmation experiment can be calculated by the expression [14]

$$CI_{CE} = \sqrt{F_{\alpha}(1, f_e) V_e \left[\frac{1}{\eta_{eff}} + \frac{1}{R} \right]} \tag{2}$$

where F_{α} is the F value for 95 % CI; f_e is the degree of freedom for error = 16 from Table 5; CI was calculated. Total degree of freedom (DOF) associated with the estimated mean = 2 + 2 + 2 + 4 = 10 and total number of experiments = 27. Effective number of replications η_{eff} is calculated using the expression $\eta_{eff} = \frac{N}{1 + \text{Total degree of freedom of mean}}$. Therefore, $\eta_{eff} = 27/(1 + 10) = 2.454$. Sample size for confirmation experiment $R = 1$. Tabulated F ratio at 95 % CI ($\alpha = 0.05$); $F = 4.49$. So $CI_{CE} = \pm 16.32$. The predicted mean of kerf width is $\mu_{kf} = 223.0 \mu\text{m}$. At 95 % CI, the predicted optimum value of kerf width is given by the expression

$$\begin{aligned} (\mu_{kf} - CI_{CE}) &< \mu_{kf} < (\mu_{kf} + CI_{CE}) \\ (223.0 - 16.3) &< \mu_{kf} < (223.0 + 16.3) \\ 206.7 &< \mu_{kf} < 239.3 \end{aligned}$$

Table 8 Response at optimum levels of process parameters

| Trial No. | Predicted mean value | Experimental value | CI |
|---------------------------|----------------------|--------------------|-----------------------------------|
| 1 | 223.0 μm | 229 μm | $206.7 < \mu_{\text{kf}} < 239.3$ |
| 2 | 223.0 μm | 227 μm | $206.7 < \mu_{\text{kf}} < 239.3$ |
| 3 | 223.0 μm | 230 μm | $206.7 < \mu_{\text{kf}} < 239.3$ |
| Average | | | |
| $K_F = 228.7 \mu\text{m}$ | | | |

Confirmation test Three confirmation tests were conducted at the optimum level of process parameters. The average mean value of kerf width is found to be within the confidence interval. The estimated error between predicted mean value and experimental average value is well within the limits of 5 % (being 2.56 % only). The experimental

values of different trials in confirmation test are reported in Table 8.

4.3 Microstructure and recast layer

To assess the kerf width measurement results, the SEM study of the machined surface is conducted. The scanning electron microscope (SEM) pictures of the machined surface of the 15 wt% $(\text{Al}_2\text{O}_3/\text{SiC})_p/\text{Al-7075}$ hybrid composite are shown in Fig. 8a–d at various levels of parameter settings. In the WEDM process, the molten material results due to the discharge energy being blasted out of the surface by the discharge pressure. This blasted material leaving the surface also resolidifies quickly due to drastic cooling by the dielectric fluid and the substrate bulk material being at room temperature. The resolidified molten metal layer, also

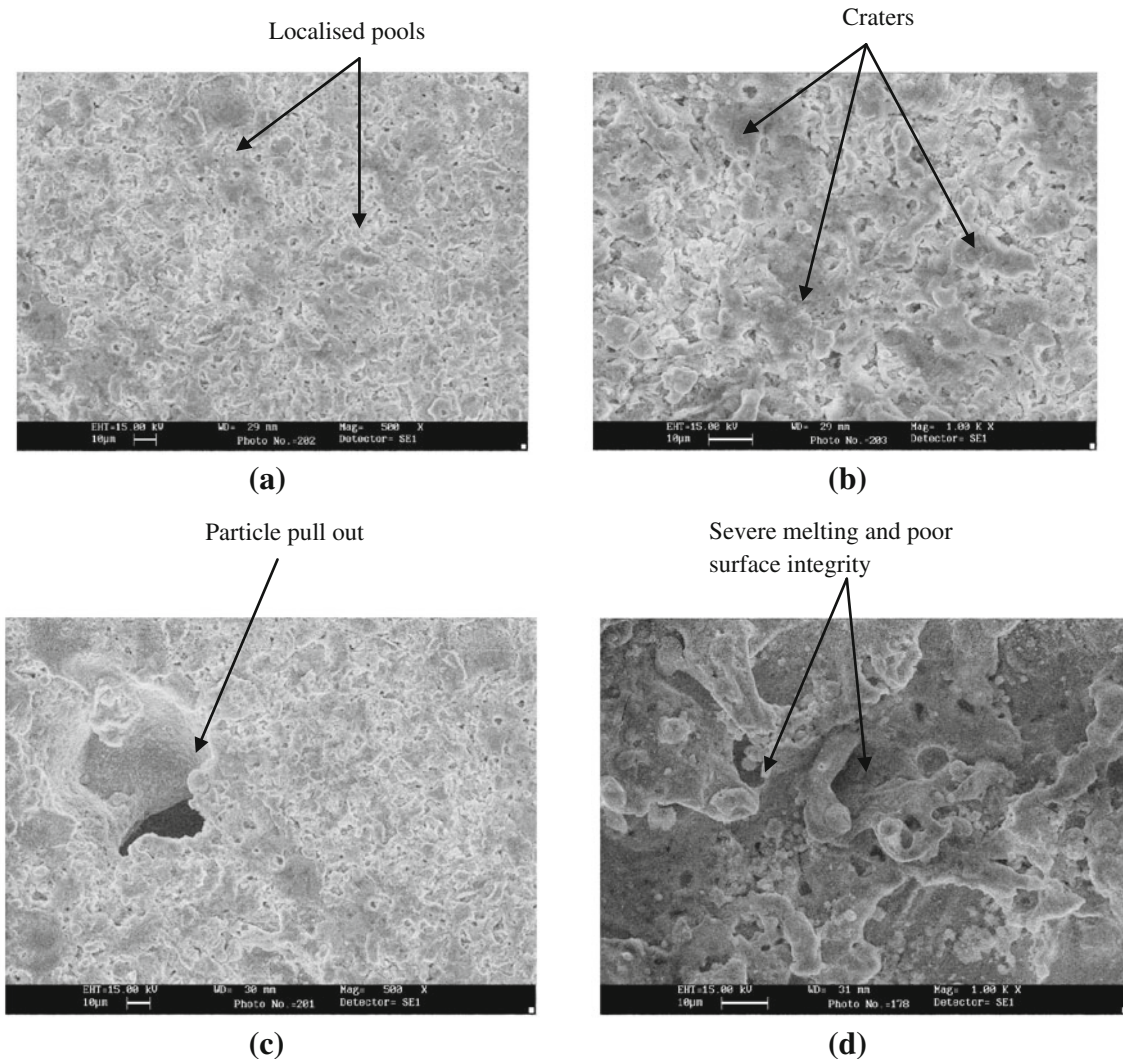


Fig. 8 SEM picture of the machined surface of 15 wt% $\text{Al}_2\text{O}_3/\text{SiC}_p/\text{Al7075}$ hybrid composite **a** $P_{\text{on}} = 4 \mu\text{s}$, $P_{\text{off}} = 2 \mu\text{s}$, $P_{\text{cur}} = 4\text{A}$, $W_s = 6 \text{ m/min}$. **b** $P_{\text{on}} = 10 \mu\text{s}$, $P_{\text{off}} = 6 \mu\text{s}$, $P_{\text{cur}} = 2\text{A}$, $W_s = 8 \text{ m/}$

min. **c** $P_{\text{on}} = 16 \mu\text{s}$, $P_{\text{off}} = 2 \mu\text{s}$, $P_{\text{cur}} = 4\text{A}$, $W_s = 6 \text{ m/min}$. **d** $P_{\text{on}} = 16 \mu\text{s}$, $P_{\text{off}} = 4 \mu\text{s}$, $P_{\text{cur}} = 6\text{A}$, $W_s = 4 \text{ m/min}$

called white layer, contains craters, globules and black patches. Figure 8a shows the machined surface at the lowest level of the parameter setting. The kerf width value is low due to less spark energy at this setting. Figure 8b shows the machined surface at moderate level setting of process parameters, indicating the moderate effect of spark energy. The close observation of the SEM picture shows discrete localized pools of the molten metal formed during machining that resolidifies on the surface. Figure 8c shows the machined surface at higher setting of the process parameters. The craters are formed by intense discharge energy. The voids and craters are also created due to reinforcement particle pullout on the machined surface. This indicates that more material melts and gets flushed out with increase in the discharge duration, discharge current and wire drum speed for the same volume fraction of reinforcements. This is because increasing the discharge duration and discharge peak current generates intense discharge energy resulting in widening and deepening of discharge craters. Figure 8(d) is the machined surface under the highest level of parameters setting having poor surface integrity, showing high volume of material melting and removal.

According to literature survey, the maximum and minimum value of kerf width produced in different materials under various settings of machining parameters are as follows: in AISI4140 steel, maximum $K_f = 380 \mu\text{m}$ and minimum $K_f = 275 \mu\text{m}$ [7], in stainless steel 304 L grade, maximum $K_f = 325 \mu\text{m}$ and minimum $K_f = 264 \mu\text{m}$ [9], in tungsten carbide maximum $K_f = 351 \mu\text{m}$ and minimum $K_f = 298 \mu\text{m}$ [10], in high strength low alloy steel maximum $K_f = 349 \mu\text{m}$ and minimum $K_f = 272 \mu\text{m}$ [11], in $\text{Al}_2\text{O}_3/\text{AA6061}$ alloy composite maximum $K_f = 450 \mu\text{m}$ and minimum $K_f = 300 \mu\text{m}$ [13]. In the current research study undertaken by the authors, the max. $K_f = 303 \mu\text{m}$ and minimum $K_f = 227 \mu\text{m}$. This shows that the newly developed $\text{AA7075/SiC/Al}_2\text{O}_3$ hybrid composite has low value of kerf width, indicating its good machining characteristic.

5 Conclusions

Hybrid metal matrix composite of 15 wt% Al_2O_3 and SiC particulates (7.5 % each) in Al-7075 alloy was prepared using inert gas-assisted electromagnetic stir-casting process. The cast hybrid composite was machined on wire EDM machine. The following conclusions are drawn

1. Hybrid composite was fabricated successfully by inert gas-assisted electromagnetic stir-casting process.
2. The linear parameters (discharge duration, discharge current and wire drum speed) and interaction

(discharge duration * discharge peak current) had significant effect on the kerf width.

3. The discharge current was the most significant parameter contributing to the kerf width (47.16 %), followed by discharge duration (38.36 %), wire drum speed (5.16 %) and interaction between discharge duration \times discharge current (5.47 %).
4. The kerf width increased with increase in discharge duration, discharge current and wire drum speed.
5. The average experimental value in the confirmation test for kerf width (228.7 μm) is found to be close to the predicted value (223.0 μm) at optimum level of input process parameters. This was within an error of 2.56 %.
6. The optimum value of process parameters for the predicted optimum value of kerf width (223.0 μm) is discharge duration 4 μs , discharge current at 2 amps and wire drum speed 4 m/min.
7. The surface topography analysis shows that high level of process parameters setting results in large amount of metal melting in the gap. This widens the kerf width.

References

1. Hung NP, Loh NN, Venkatesh VC (1999) Machining of metal matrix composites, Machining of ceramics and composites. Marcel Dekker, New York, pp 295–298
2. Groover MP (2004) Fundamental of modern manufacturing: materials, processes, and systems, 2nd edn. John Wiley & Sons, New Jersey
3. Poon SK, Lee TC (1993) Electrical discharge machining of particulate metal matrix composites. Proc. ASM Materials Congress, Pittsburgh, pp 43–50
4. Brahmankar PK, Ramkrishnan N (2005) On the fatigue characteristics of electro-discharge machined alumina particulate reinforced aluminium matrix composites. Int J Manuf Technol Manag 7(2):342–351
5. Dauw DF, Brown CA (1990) Surface topography investigations by fractal analysis of spark-eroded electrically conductive ceramics. Ann CIRP 37(2):161–165
6. Scott D, Boyina S, Rajurkar KP (1991) Analysis and optimisation of parameter combination in wire electrical discharge machining. Int J Prod Res 29(11):2189–2207
7. Nihat Tosun, Can Cogun, Gul Tosun (2004) A study on kerf and material removal rate in wire electrical discharge machining based on Taguchi method. J Mater Process Technol 152:316–322
8. Yan BH, Tsai HC, Huang FY, Lee LC (2005) Examination of wire electrical discharge machining of $\text{Al}_2\text{O}_3\text{p}/6061\text{Al}$ composites. Int J Mach Tools Manuf 45:251–259
9. Parashar V, Rehman A, Bhagoria JL, Puri YM (2010) Kerfs width analysis for wire cut electro discharge machining of SS 304L using design of experiments. Indian J Sci Technol 3:4
10. Shah A, Mufti Nadeem A, Rakwal Dinesh, Bamberg Eberhard (2011) Material removal rate, kerf, and surface roughness of tungsten carbide machined with wire electrical discharge machining. J Mater Eng Perform 20:71–76

11. Gupta P, Khanna R, Gupta RD, Sharma N (2013) Effect of process parameters on kerf width in WEDM for HSLA using response surface methodology, *J Eng Technol* 2(1):1–6
12. Yang RT, Tzeng CJ, Yang YK, Hsieh MH (2012) Optimization of wire electrical discharge machining process parameters for cutting tungsten. *Int J Adv Manuf Technol* 60:135–147
13. Patil NG, Brahankar PK (2010) Some studies into wire electro-discharge machining of alumina particulate-reinforced aluminum matrix composites. *Int J Adv Manuf Technol* 48:537–555
14. Ross PJ (1996) Taguchi techniques for quality engineering. Mc Graw-Hill, New York